MULTI-THERMAL OBSERVATIONS OF NEWLY FORMED LOOPS IN A DYNAMIC FLARE

ZDENĚK F. ŠVESTKA

Laboratory for Space Research Utrecht, SRON, The Netherlands

JUAN M. FONTENLA

IAFE, Buenos Aires, Argentina. Presently NAS/NRC Research Associate, Space Science Laboratory, NASA MSFC, U.S.A.

MARCOS E. MACHADO*

Space Science Laboratory, NASA MSFC, Huntsville, AL 35812, U.S.A.

SARA F. MARTIN

Solar Astronomy, CALTECH, Passadena, CA 91125, U.S.A.

DONALD F. NEIDIG

*Air Force Geophysics Laboratory, National Solar Observatory, Sacramento Peak**, Sunspot, NM 88349, U.S.A.*

and

GIANNINA POLETTO

Osservatorio Astrofisico di Arcetri, Firenze, Italy

(Received 7 November, 1986; in revised form 10 February, 1987)

Abstract. The dynamic flare of 6 November, 1980 (max $\approx 15:26$ UT) developed a rich system of growing loops which could be followed in Hα for 1.5 hr. Throughout the flare, these loops, near the limb, were seen in emission against the disk. Theoretical computations of deviations from LTE populations for a hydrogen atom reveal that this requires electron densities in the loops close to, or in excess of 10^{12} cm^{-3}. From measured widths of higher Balmer lines the density at the tops of the loops was found to be 4×10^{12} cm^{-3} if no non-thermal motions were present, or 5×10^{11} cm^{-3} for a turbulent velocity of ~ 12 km s^{-1}.

It is now general knowledge that flare loops are initially observed in X-rays and become visible in Hα only after cooling. For such a high density, a loop would cool through radiation from 10^7 to 10^4 K within a few minutes so that the dense Hα loops should have heights very close to the heights of the X-ray loops. This, however, contradicts the observations obtained by the HXIS and FCS instruments on board SMM which show the X-ray loops at much higher altitudes than the loops in Hα. Therefore, we suggest that the density must have been significantly lower when the loops were formed and that the flare loops were apparently both shrinking and increasing in density while cooling.

1. Introduction

For quite some time, the dynamic flare of 6 November, 1980 (max $\approx 15:26$ UT) was a puzzle for us. Close to the eastern solar limb, it developed a rich system of Hα loops,

* NAS/NRC Research Associate, on leave from CNIE, Argentina.

** Operated by the Association of Universities for Research in Astronomy, Inc., under contract with the National Science Foundation. Partial support for the National Solar Observatory is provided by the USAF under a Memorandum of Understanding with the NSF.

Solar Physics **108** (1987) 237–250.

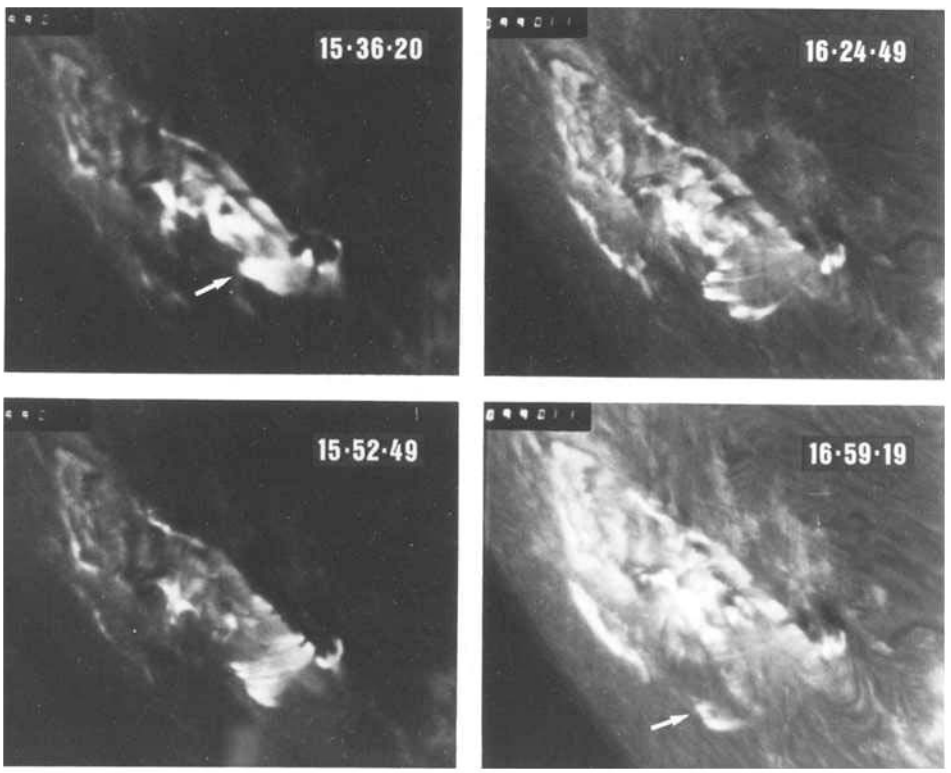

Fig. 1. High-resolution Hα photographs of the growing loop system on 6 November, 1980. (Big Bear Observatory, Caltech.) UT is given on the frames.

the tops of which were conspicuously rising from a projected altitude of 25 000 to 55 000 km for 90 min, and all the time the loops, projected on the solar disk, were in emission. Figure 1 shows examples of the growing loop system at four different times, selected from a high-resolution Hα movie made at Big Bear Solar Observatory. These are pictures in the Hα line center, but even at 1 Å off-band, filtergrams obtained at the US Air Force Solar Optical Observing Network Ramey station show that the tops of the loops were in emission since their first appearance at 15 : 28 UT through at least 16 : 28 UT (the last available off-band photograph). In the line centre, the emission loops could be seen until 17 : 05 in the Big Bear movie (becoming too weak to be seen after that). There are other dynamic flares in which loops appear in emission for a short period of time, usually close to the beginning of their growth, but loops persisting in emission for more than 90 min seem to be an extraordinary event.

According to Zirin (1987, and private communication) the loop appearance in emission requires electron density in excess of 10^{12} cm^{-3} in the emitting loops – very high in comparison to other observations of loops in dynamic flares (which are usually called, rather incorrectly, post-flare loops). Moore *et al.* (1980), for example, give densities of 4×10^{10} to 10^{11} cm^{-3} in the early phase of the development of a loop system,

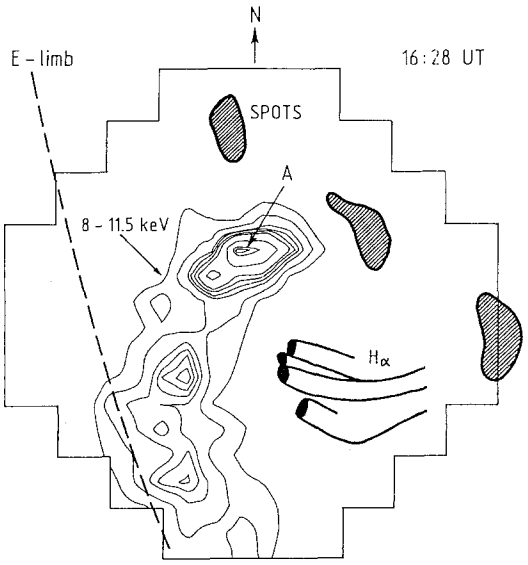

Fig. 2. HXIS image of the tentative tops of the X-ray (post-)flare loops at 16:28 UT (in 8.0–11.5 keV X-rays). Below them (note the proximity to the limb) the Hα loops are indicated as they looked at the same time in the Big Bear movie (cf. Figure 1). The Hα loops started to grow one hour earlier, at 15:28 UT. The X-ray feature 'A' was another element of the flare, stationary and long-lived, and had no apparent relation to the growing loop system of the dynamic flare.

decreasing to 10^{10} cm^{-3} one and a half hours later. Similar densities were found for another dynamic flare by Švestka *et al.* (1982); note that according to Švestka and Poletto (1985) the real loop density was probably still smaller than given there, by a factor of 2 to 4).

It is generally assumed (e.g., Moore *et al.*, 1980) that a newly excited (or rather newly formed) very hot loop, initially visible in X-rays, stays at the same altitude and cools there until we begin to see it in Hα. If Zirin were correct that loops in Hα emission require density $> 10^{12}$ cm^{-3}, then, assuming a similar density for the loops in the 6 November flare, radiation would cool the hot plasma from 10^7 K to the chromospheric temperature of 10^4 K in less than two minutes (cf. Section 3). Thus, considering the slow growth rate of the loops (cf., e.g., Figure 7), we should see hot loops in X-rays at about the same altitude as the Hα loops. Instead, as Figure 2 demonstrates, the X-ray emission was seen much higher than the tops of the Hα loops. In fact, the observed growth rate of the loop system and the observed separation between the hot and cool components indicate that more than one hour is required for the loops to become visible in Hα at the same place where they were seen as X-ray loops. Thus we encountered clear discrepancy which required a more detailed analysis of the event.

2. Density of the Loops

2.1. Computations

The density given by Zirin was based on a comparison of estimated collisional and radiative excitation rates, without any detailed computations. So we first tried to verify

Zirin's statement by computing the expected deviations from the LTE populations of the second and third quantum levels in a hydrogen atom (the *b*-factors) for various temperatures and densities.

We have assumed a plane parallel infinite slab with thickness z along the line-of-sight. We then solve the equations for a 3-level plus continuum hydrogen atom, with detailed solution of all transitions, considering the statistical equilibrium and radiative transfer equations for a set of constant pressures and temperatures representative of the expected range of values of these quantities in flares. The method we have used was described earlier by Fontenla and Rovira (1985a, b).

For any pressure p, assumed to vary within the range of $0.2 < p < 10$ dyn cm^{-2}, and defined as

$$p = (n_e + n_i + n_1 + n_2 + n_3)\, kT\,, \tag{1}$$

where n_e, n_i are electron and ion density, and n_1, n_2, n_3 are the populations of the lowest three levels of the hydrogen atom, we considered three different values of T, namely $T = 8000$, 10 000, and 15 000 K.

For the incident radiation in the 3–2 transition (i.e., Hα) we use a dilution factor $W = 0.45$, which takes into account the center-to-limb variation of the incident Hα intensity 'seen' by a prominence or (post-)flare loop (Fontenla, 1979). Similarly, we adopt $W = 0.40$ for Lα and Lβ, with corresponding radiation temperatures $T_r = 7400$ and 6800 K, as suggested by the OSO–8 observations (Gouttebroze *et al.*, 1978; Lemaire *et al.*, 1981). In the Lyman continuum we have used the Skylab data, and approximated the incident intensity by

$$I_\nu = W \frac{2h\nu^3}{c^2} \frac{r^{-1}}{\exp(h\nu/kT_c) - 1}\,, \tag{2}$$

with $T_c = 8000$ K, $W = 0.4$, and $r = 180$. The factor r is needed to fit the brightness temperature in the Lyman continuum as observed by Vernazza and Reeves (1978): $I_\nu = B_\nu(T_c)/r$, where T_c is the colour temperature. The background intensity at $\lambda_0 + 1$ Å in Hα, at $\mu = 0.3$, is taken as $I_{\nu 1} = 1.81 \times 10^{-5}$ erg cm^{-2} s^{-1} sr^{-1} Hz^{-1} (White, 1964).

The results, for $z = 1000$ km and zero turbulent velocity are shown in Table I. One can see there that, generally, the loops change from absorption to emission as soon as the plasma pressure exceeds ≈ 3 dyn cm^{-2}. For an average Hα flare-loop temperature of 10^4 K this pressure value implies an approximate electron density of 10^{12} cm^{-3}, in full agreement with Zirin's estimate.

Quite recently, after the preliminary results of our analysis had been presented at the SMA Symposium in Toulouse (Švestka *et al.*, 1986), Heinzel and Karlický (1986, and private communication) showed us results of their independent computations of the Hα radiation coming from tops of loops extending 50 000 km high in the corona. Though their approach differed from ours in several points, they got very much the same results as we did: the electron density must exceed a limit of $\sim 10^{12}$ cm^{-3} to make the loops change from absorption to emission when projected on the solar disk.

TABLE I

The occurrence of flare loops in absorption or emission in dependence on temperature and density

T (K)	P (dyn cm^{-2})	b_1	b_2	b_3/b_2[a]	n_e (cm^{-3})	Appearance[b]
8000	0.2	55.0	33.0	3.02E − 2	6.5E + 10	abs.
	1.0	7.07	7.17	6.64E − 2	3.6E + 11	abs.
	2.0	3.91	3.98	1.86E − 1	7.0E + 11	abs.
	3.0	2.51	2.55	3.40E − 1	1.1E + 12	em.
	5.0	1.55	1.56	6.10E − 1	1.8E + 12	em.
	7.0	1.25	1.26	7.75E − 1	2.4E + 12	em.
	10.0	1.11	1.11	8.92E − 1	3.3E + 12	em.
10000	0.2	1140	308	2.00E − 2	6.5E + 10	abs.
	1.0	49.8	30.1	6.15E − 2	3.5E + 11	abs.
	2.0	14.6	9.90	1.39E − 1	7.1E + 11	barely em.
	3.0	7.37	5.29	2.27E − 1	1.1E + 12	em.
	5.0	3.32	2.61	4.10E − 1	1.8E + 12	em.
	7.0	2.09	1.78	5.73E − 1	2.5E + 12	em.
	10.0	1.41	1.32	7.58E − 1	3.6E + 12	em.
15000	0.2	1.40E + 5	5140	1.01E − 2	4.7E + 10	abs.
	1.0	5850	818	5.24E − 2	2.4E + 11	abs.
	2.0	1550	267	1.22E − 1	4.8E + 11	em.
	3.0	748	128	1.84E − 1	7.2E + 11	em.
	5.0	316	48.6	2.80E − 1	1.2E + 12	em.
	7.0	182	25.7	3.50E − 1	1.7E + 12	em.
	10.0	107	13.5	4.32E − 1	2.4E + 12	em.

[a] 2.00E − 2 = 2.00 × 10^{-2}.

[b] Here we simply compare the resulting source function with the background intensity. As we point out in Section 2.2, one actually cannot see the loops either in emission or absorption at $\Delta\lambda$ = 1.0 Å unless their optical thickness at this $\Delta\lambda$ is enhanced by turbulence.

We also repeated our computations for other values of z (100 and 10000 km) and for turbulent velocities up to 12 km s^{-1}, with essentially the same results as concerns the conditions for the Hα loop emission. (That means, e.g., that there may be a significant change in the absolute values of the b-factors, but not in their ratios.) As can be noted from the parameters chosen for Equation (2) and Hα intensity, the calculations were made for quiet Sun background radiation field. This seems to be justified in the present case considering the absence of strong Hα emission from flare ribbons in this particular event (cf. Figure 1). Yet, we still performed additional test runs increasing the Hα background field by up to a factor 2, and the Lyman continuum and Lyman lines intensity up to a factor 10, with the result that the maximum increases in the b_3/b_2 ratios of Table I stayed below 4%.

More significant perhaps may be the effect of ionizing radiation from the overlying, newly formed, soft X-ray loops. It is difficult to take this effect into account, due to the lack of appropriate data and, therefore, it was not included in our calculations (nor in the computations made by Heinzel and Karlický). However, recent computations of flare model atmospheres including strong soft X-ray fluxes (Avrett and Machado, paper in preparation) have shown only minor changes in the hydrogen-ionization balance.

The Doppler brightening effect cannot be important here, because the loops moved almost entirely in a lateral direction and no observable differences could be detected in the off-band data. Besides, this effect should be predominantly in the loop legs, where Hα material often is seen falling down, not at the loop tops. But just the loop tops were the parts seen in emission all the time.

2.2. Observations

The calculated density can be checked by tracing the Balmer line spectrum of the top part of the loops obtained at Sacramento Peak at 15:46 UT (18 min after the first visibility of the Hα loops). The observed H_7 and H_8 Balmer lines had total halfwidths of 0.40 and 0.36 Å, respectively, while the H_9 line was already too weak to produce any detectable emission. Therefore, we are allowed to assume that the H_8 line was optically thin, and determine the electron density at the tops of the loops from its halfwidth.

The broadening mechanisms to be considered are Doppler broadening and Stark effect. By using de Feiter's (1966) computations and assuming $T = 10^4$ K, one finds $n_e = 4 \times 10^{12}$ cm^{-3} if no non-thermal motions were present. From Kurochka's (1969) tables one gets $n_e = 5 \times 10^{12}$ cm^{-3} for $T = 8 \times 10^3$ K.

However, the assumption of zero non-thermal motions is not realistic because in such a case the Hα line could not be broad enough to produce observable emission at $\Delta\lambda = 1.0$ Å as it was observed at the SOON Ramey Station. With purely thermal Doppler broadening at $T = 10^4$ K, without any non-thermal motions, the optical thickness at $\Delta\lambda = 1.0$ Å is only $\tau(1.0) = 3 \times 10^{-6}\, \tau(0)$. It is true that the filter passband used at Ramey Station was 0.5 Å, so that emission at ~ 0.8 Å from the line center could be responsible for the emission observed at 1.0 Å, but even then, without any non-thermal contribution and with temperature $T = 10^4$ K the optical thickness is too small: $\tau(0.8) = 3 \times 10^{-4}\, \tau(0)$.

Thus it is necessary to assume some turbulence at the top of the loops. From Kurochka's (1969) tables, the halfwidth of the H_8 line should be 0.12 Å for $n_e = 5 \times 10^{11}$ cm^{-3} if no non-thermal motions were present. Thus, with $n_e = 5 \times 10^{11}$ cm^{-3} and the observed halfwidth of 0.18 Å we can make allowance for a turbulent velocity $V_t = 13.1$ km s^{-1} for $T = 8 \times 10^3$ K and 11.7 km s^{-1} for $T = 10^4$ K. In that case, the Doppler width in the Hα line increases from 0.25–0.28 Å to 0.38 Å which yields $\tau(1.0) = 10^{-3}\, \tau(0)$ and $\tau(0.8) = 0.012\, \tau(0)$.

The fact that H_8 was the highest discernible line leads, using de Feiter's (1966, p. 46) results, to $n_2 z = 4 \times 10^{13}$ cm^{-2}, a value that is entirely consistent with our present calculations; for example, for the $p = 3.0$ dyn cm^{-2}, $T_e = 10^4$ K model we obtain $n_2 z = 6 \times 10^{13}$ cm^{-2}. We recall that this value applies to the tops of the flare loops; in chromospheric flare ribbons, at the footpoints of flare loops, the electron density is always found to be in excess of 10^{13} cm^{-3} and the highest discernible line is usually H_{13} (Švestka, 1976), leading to $n_2 z > 8 \times 10^{14}$ cm^{-2}. Thus the $n_2 z$ value along the line-of-sight through the top of the flare loops is more than 20 times smaller than in the flare parts deep in the chromosphere as it is to be expected.

With the value of $n_2 z = 4 \times 10^{13}$ cm^{-2} one finds in the Hα line center $\tau(0) = 29$.

Thus, $\tau(1.0) = 0.03$ and $\tau(0.8) = 0.35$, which can explain the observed emission seen at 1.0 ± 0.25 Å.

Finally, let us check how this $\tau(0)$ in the Hα line agrees with our original assumptions on the τ values in the higher Balmer lines: we get $\tau(0) = 0.50$ in the H_7 line (so that some self-absorption and, in consequence of it, a larger halfwidth of 0.40 Å is to be expected), $\tau(0) = 0.27$ in the H_8 line (which makes our assumption of an optically thin line acceptable) and $\tau(0) = 0.16$ in the H_9 line (which can explain its invisibility). A slightly smaller value of $n_2 z$ (by about a factor 2) might fit better, but the agreement is pretty good when all the uncertainties involved are taken into account.

Thus, strictly speaking, the observed higher Balmer lines do not prove that the electron density at the tops of the loops was of the order of 10^{12} cm^{-3}, because we do not know the real contribution of turbulent motions to the line broadening; the spectrum shows, however, that the observations are consistent with such a high electron density, provided that non-thermal motions at the loop tops were relatively small. One would certainly expect turbulence at the tops of the loops, especially if the loops are newly formed through a reconnection process, like in the Kopp and Pneuman (1976) model. However, one can also suppose that any such turbulence might significantly decay before the loops become visible in the Hα line, long after their formation. Turbulence may be easily damped in the high-density plasma of the low-temperature loops.

3. Cooling of the Loops

A loop which has been newly formed high in the corona will cool through conduction and radiation. Assuming classical conduction, temperature gradient $\nabla T = T/L$ (where L is the half-length of the loop), and radiative cooling from Raymond *et al.* (1976), one finds that a loop at an altitude of $\approx 50\,000$ km and $T = 10^7$ K needs about 1 hr to cool to the Hα temperature if its electron density is 10^{10} cm^{-3}. For an electron density $n_e = 10^{11}$ cm^{-3} the cooling time is about 10 min, and for $n_e = 10^{12}$ cm^{-3} it decreases to only slightly more than 1 min (Švestka, 1987). In this latter case conduction is negligible and the loops cool only through radiation which cannot be inhibited. Thus we see that the high X-ray loops in Figure 2 either must have had a density much lower than 10^{12} cm^{-3}, or they must bear no relation to the loops seen in Hα, i.e., the Hα loops are not the cool remnants of loops previously seen in X-rays (as assumed, e.g., by Moore *et al.* (1980) and elsewhere).

4. Observations in X-ray Lines

In order to check whether the Hα loops and the X-ray enhancement in Figure 2 were related phenomena, we have used images of the flare in various X-ray lines provided by the Flat Crystal Spectrometer (FCS) of the XRP experiment aboard the SMM. Table II summarizes the lines we have used: $T(o)$ is the optimum temperature for the line formation, $T(m)$ is the minimum temperature which yields 10% of the maximum flux.

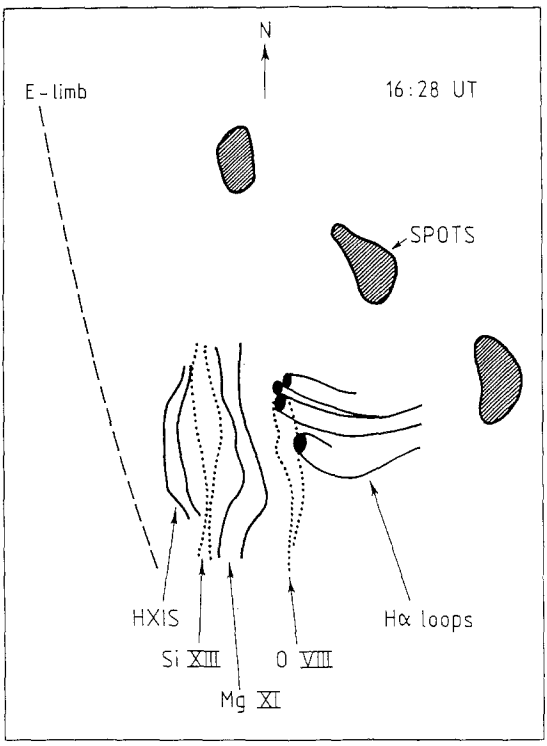

Fig. 3. Images of the tops of the loops in different X-ray lines of the FCS (O VIII, Mg XI, Si XIII) compared with the Hα loops and the median of HXIS contours from Figure 2 (same time). Medians for the X-ray lines were constructed in the same way as for HXIS, i.e., we found the centroids of all contours in the east–west direction and drew an envelope of all the points thus obtained.

In every FCS image we determined, for the area overlying the Hα loops, the median of each intensity isocontour along the east-west direction (which was the direction of the growing Hα loops) and drew the envelope of these medians. We obtained thus the median contours shown in Figure 3, for the time of Figure 2. The highest (farthest eastwards) contour is the median of the HXIS contours shown in Figure 2.

TABLE II

List of used FCS X-ray lines

Ion	$T(m)$	$T(o)$
O VIII	1.7×10^6 K	2.9×10^6 K
Mg XI	2.8	6.2
Si XIII	4.4	9.5
Fe XXV	20	60
Hα	$< 2.0 \times 10^4$ K	
HXIS	$> 10 \times 10^6$ K	

The sequential positions of these median contours give clear evidence that what we see as the HXIS image in Figure 2 really are the flare loops. The altitude of the loops is successively higher with increasing temperature, from the 'cool' O VIII loops which practically coincide with the Hα loops, through the hotter lines of Mg XI and Si XIII up to the 'very hot' HXIS contours which are practically identical with the Fe XXV median. Thus the loops must cool quite slowly from the high temperatures ($T > 10^7$ K) of the Fe XXV and HXIS emission to the $T \approx 2 \times 10^6$ K of O VIII, but quite rapidly from $T \approx 2 \times 10^6$ K to the chromospheric temperature.

5. Shrinking of the Loops

The procedure described in the previous paragraph and applied at different times allowed us to determine the temporal variation of the projected altitudes of the loops in the various lines above the footpoints of the Hα loops. The result is shown in Figure 4. For more than 2 hours the hot X-ray loops extend continuously much higher than the Hα loops. (After 17 : 00 UT we assume that the cool loops can be traced from the O VIII images, as Figure 4 indicates can be done prior to that time.)

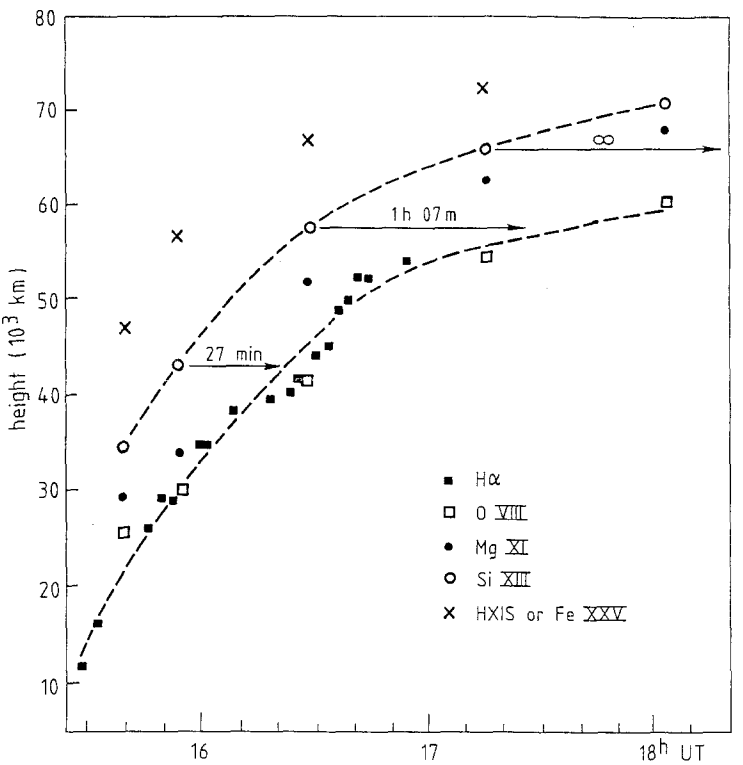

Fig. 4. Time-variation of the measured altitude of the flare loops in Hα, X-ray lines corresponding to different temperatures (cf. Table II), and HXIS (or Fe XXV which yields very similar images). Two dashed curves follow the growth of the loop system at low temperatures (Hα and O VIII) and at $\approx 10^7$ K (Si XIII), respectively. Arrows and times show cooling of stationary loops (cf. text).

If we were to follow the procedure in Moore *et al.* (1980) we would assume that a new loop is formed at a given altitude and stays there, gradually cooling. Then the corresponding cooling times (arrows in Figure 4) would be 27 and 67 min at 15 : 58 and 16 : 28 UT, respectively, but would apparently grow to infinity after 17 : 20 UT, because the cool loops seem to be unable to reach the altitude of the hot loops after this time. A look at Figure 8.5 in Moore *et al.* shows that the situation in the dynamic flare of 28 July, 1973 was very similar: the cool loops could never reach the altitudes on which the late hot X-ray loops were seen.

From this behaviour one can conclude that those newly formed hot loops which later become visible in Hα cannot cool at their original altitudes, but have to shrink to lower heights before they are seen in the Hα line. Figure 5 shows the alternatives, for a sample loop seen at 16 : 28 UT in the Si XIII ($T \approx 10^7$ K) line in Figures 3 and 4. Assuming no shrinking, and cooling at constant density, a cooling time of 1h07m would imply a low density of 4×10^9 cm^{-3} (horizontal track in Figure 5). At the other extreme, if the density of this loop were 10^{12} cm^{-3}, as the Hα loops indicate, it would cool in less than two minutes (nearly vertical track) and become visible at 16 : 30 UT as an Hα loop. This seems unlikely, because with such a cooling rate the lifetime of the hot loops

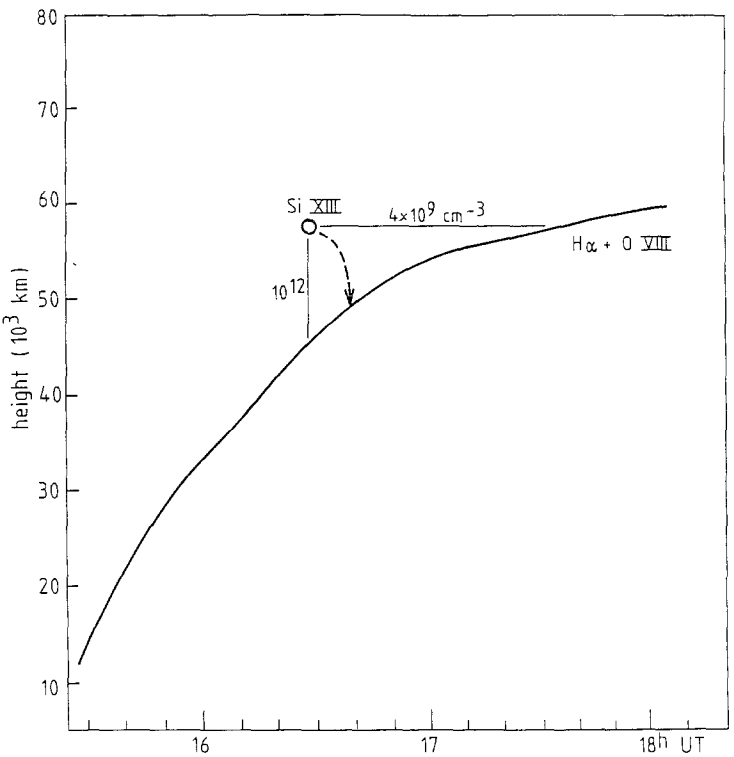

Fig. 5. Various possible cooling paths of a 10^7 K loop seen at 16 : 28 UT in Figures 3 and 4. Numbers on the linear cooling paths give the constant densities appropriate to each path. See text for an explanation of the dashed arrow.

would be extremely short and we could see them only in case that new loops were being continuously formed throughout the whole duration of the flare.

Alternately, the real path of the loop top from the Si XIII position to the Hα position in Figure 5 must be somewhere in between, as the dashed arrow indicates: the altitude of the loop decreases gradually, while simultaneously the plasma density in the loop increases and the cooling time becomes progressively shorter. Computations of various expected paths, with variable starting densities and density-increase functions, are presently being made by Kopp and Poletto.

6. Discussion

The referee of this paper has pointed out that the shrinking of the hot loops requires that the plasma β (ratio of gas pressure to magnetic pressure) is greater than unity. Without any additional plasma inflow this would imply that more than half of the magnetic energy is converted into plasma energy as field lines reconnect and new loops are formed. This, however, apparently does not happen, since it is more likely that the density begins to increase only later on, in consequence of the evaporation of chromospheric gas. Thus the shrinking is not directly related to the reconnection process itself. Under this assumption Figure 6 shows the scenario of the loop formation we propose.

As a starting point we adopt the Kopp and Pneuman (1976) model of the field opening and subsequent field-line reconnections. Immediately after reconnection we envisage that a cusp-shaped non-potential loop is formed (Figure 6(a)) which subsequently shrinks to a quasi-potential configuration without a cusp. The prevailing opinion among theorists is that this transition to the quasi-potential configuration will be fast. Eventually one gets a potential loop below, and another component resembling an inverted coronal arch above (Figure 6(b)). Through a reconnection-associated shock, particle streams, and/or heat conduction, chromospheric material will evaporate into the hot X-ray loop.

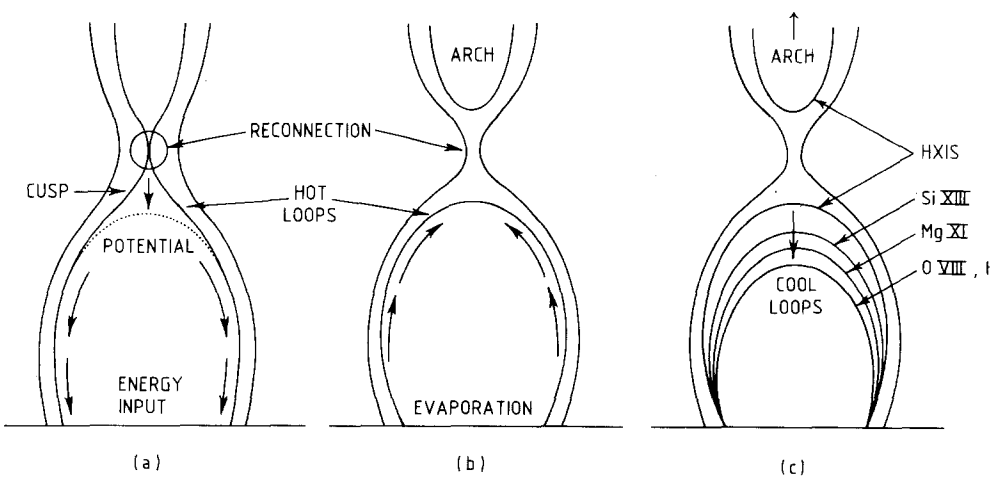

Fig. 6a–c. A tentative scenario of the loop formation. See discussion in the text.

This will lead to an enhancement of the loop density and the loop is first expected to expand (Kopp and An, private communications), because of momentum flux of the plasma injected from below. However, if the loop becomes very dense, and thus very heavy, the gravitational forces will cause the loop to collapse and seek a different equilibrium configuration at a lower altitude (An, private communication; partly An *et al.*, 1986). This will occur after a time which depends on the injection velocity, plasma density, and magnetic strength of the loop formation, i.e., quantities we do not know.

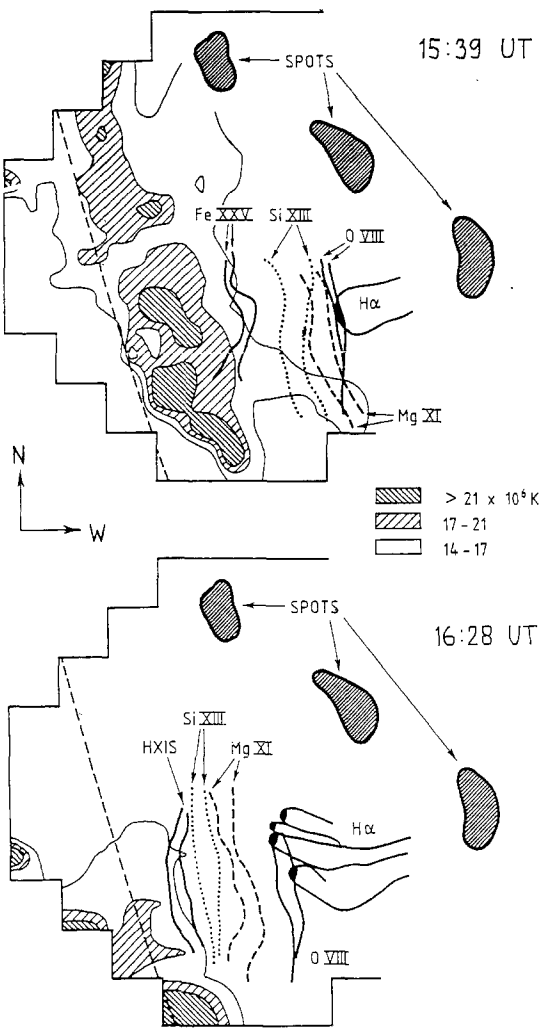

Fig. 7. A comparison of the growth of the loop system (in Hα, O VIII, Mg XI, Si XIII, and Fe XXV or HXIS data) with the upward motion of the maximum of temperature in the corona (T determined from the ratio of counts in the 3.5–5.5 keV and 5.5–8.0 keV energy bands of HXIS). The eastern solar limb is marked by a dashed curve. The upper image corresponds to 15 : 39 UT for the loops and 15 : 46 UT ($\pm$ 9 min of integration) for the thermal map. The lower image corresponds to 16 : 28 UT for the loops (same as Figure 3) and 16 : 30 UT ($\pm$ 8 min of integration) for the thermal map.

The collapse will be accompanied by compression and, thus, by further density increase. As the density increases, the loop would then pass through the different temperature regimes characterizing HXIS, FCS, and, eventually, Hα observations (Figure 6(c)).

Finally, to verify that the Kopp and Pneuman model, which we have adopted, can be applied to this particular flare, we have compared the apparent rise of the loop system in the various X-ray lines with the speed of the rising thermal disturbance ('thermal wave') detected by Švestka (1985; also see Hick and Švestka, 1987) in the same flare event. This moving temperature maximum in the corona (Figure 7) is supposed to correspond to an upward motion of the 'arch' in Figure 6. The speed of this motion, between 15 : 43 and 16 : 36 UT, was 7.4 km s^{-1}. The average speed of the loop system between 15 : 39 and 16 : 28 UT, for comparison, was 7.7 km s^{-1} in the Si XIII line and 8.3 km s^{-1} in Hα. Both speeds thus seem to correspond to the speed of the rising reconnection point common to both the arch and the loops, and strongly support our initial assumption that the loops form through a series of magnetic field reconnections.

Acknowledgements

The FCS data used in this analysis was kindly provided by Mr Kermit Smith and Ramey Hα images by Dr Dave Rust. We acknowledge several stimulating discussions with Dr Petr Heinzel during his visit at the NASA Goddard Space Flight Center and during his stay in Utrecht. Also an interesting comment by the referee has been appreciated. This research is a part of the SMM Guest Investigator Program of Z. Švestka who acknowledges the financial support from SRON in The Netherlands and from CNR in Italy. The contribution of S. F. Martin was supported by contracts N0014–84–K–0412 and N0014–86–K–0139 from the Office of Naval Research, USA. The authors thank Hans Braun in Utrecht for drawing the figures.

The SMM spacecraft was repaired in orbit by the crew of Challenger on mission 41-C. The pilot of the mission, and the commander of Challenger's last mission was Francis R. Scobee. This work is dedicated to his memory.

References

An, C. H., Bao, J. J., and Wu, S. T.: 1986, in A. I. Poland (ed.), Proc. SMM Workshop on Coronal and Prominence Plasmas, p. 51.

De Feiter, L. D.: 1966, 'Analysis of the Balmer Spectrum of Solar Flares', Thesis, University Utrecht.

Fontenla, J. M.: 1979, *Solar Phys.* **64**, 177.

Fontenla, J. M. and Rovira, M. G.: 1985a, *Solar Phys.* **96**, 53.

Fontenla, J. M. and Rovira, M. G.: 1985b, J. Quant. Spectr. Rad. Trans. **34**, 389.

Gouttebroze, P., Lemaire, P., Vial, J. C., and Artzner, G. E.: 1978, *Astrophys. J.* **225**, 655.

Heinzel, P. and Karlický, M.: 1986, paper presented at Solar Conf. in Stará Lesná, Czechoslovakia, September 1986. (Also see 1987, *Solar Phys.*, in press.)

Hick, P. and Švestka, Z.: 1987, *Solar Phys.* **108**, 315 (this issue).

Kopp, R. A. and Pneuman, G. W.: 1976, *Solar Phys.* **50**, 85.

Kurochka, L. N.: 1969, *Astron. Zh.* **46**, 85.

Lemaire, P., Gouttebroze, P., Vial, J. C., and Artzner, G. E.: 1981, *Astron. Astrophys.* **103**, 160.

Moore, R., McKenzie, D. L., Švestka, Z., Widing, K. G., and 12 co-authors: 1980, in P. A. Sturrock (ed.), *Solar Flares*, Skylab Solar Workshop II, p. 341.
Raymond, J. C., Cox, D. P., and Smith, B. W.: 1976, *Astrophys. J.* **204**, 290.
Švestka, Z.: 1976, *Solar Flares*, D. Reidel Publ. Co., Dordrecht, Holland.
Švestka, Z.: 1985, *Adv. Space Res.* **4**, No. 7, 179.
Švestka, Z.: 1987, *Solar Phys. (Letter)* **108**, 411 (this issue).
Švestka, Z. and Poletto, G.: 1985, *Solar Phys.* **97**, 113.
Švestka, Z., Dodson-Prince, H. W., Martin, S. F., Mohler, O. C., Moore, R. L., Nolte, J. T., and Petrasso, R. D.: 1982, *Solar Phys.* **78**, 271.
Švestka, Z., Fontenla, J. M., Machado, M. E., Martin, S. F., Neidig, D. F., and Poletto, G.: 1986, *Adv. Space Res.* **6**, No. 6, 253.
Vernazza, J. E. and Reeves, E. M.: 1978, *Astrophys. J. Suppl.* **37**, 485.
White, O. R.: 1964, *Astrophys. J.* **139**, 1340.
Zirin, H.: 1987, *Astrophysics of the Sun*, Cambridge Univ. Press, Cambridge.